Modeling of BVA Resonator for Collective Fabrication

A. Clairet[1], T. Laroche[2], L. Couteleau[1], and J.J. Boy[3]

[1]*RAKON FRANCE, 2 rue Robert Keller, 10150 Pont-Sainte-Marie, FRANCE*

[2]*FEMTO-ST, UMR 6174, Frequency & Time Dept, 26 chemin de l'Epitaphe, 25000 Besançon, FRANCE*

[3]*ENSMM/FEMTO-ST, Frequency & Time Dept, 26 chemin de l'Epitaphe, 25000 Besançon, FRANCE*

***Abstract*— In this paper, we report on the use of Finite Elements Software to model and simulate new resonator designs, working at about 9 MHz. We aim to review the concept of BVA resonator by reducing the size. The miniaturization of the whole resonator will allow us to use collective processes and therefore reduce the cost of manufacturing. To achieve this result, we investigated to replace the radius of curvature, necessary for a good trapping of the vibrating energy at this frequency, by several mesas.**

I. Introduction

High quality resonators are only made by unitary way. In order to allow a better integration in electronic system but also and especially a lower cost of manufacturing by performing collective processes [1], we investigated a way to reduce the size of these resonators while maintaining at least the same performances. Therefore, we tried to discretize the radius of curvature and replace it by a series of steps (cf. Fig. 1).

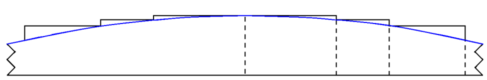

Fig. 1. Example of discretization

We focus our study on SC-cut quartz resonator for which its C-mode 3^{rd} overtone is vibrating at about 10 MHz. Computations have been done with COMSOL Multiphysics® on the "Mesocentre de calcul de Franche-Comté machine".

II. Resonator with radius of curvature

The resonator has a diameter of 14 mm and a thickness of 600 μm. We apply an electrical potential by using gold electrodes with a diameter of 7 mm and a thickness of 200 nm. With this configuration, we seek the radius of curvature which gives the best quality factor. The results obtained with various radii are summarized in the table I and displacements obtained for some of them are ploted in the Fig. 2 along the projection in the plane of the x-axis.

Even if the quality factor evolves according to the different designs, it remains around 1.5 million (the Q.f product is equal to 1.36e13).

The acoustic loss is evaluated by introducing the tensor of viscosity constants measured by Lamb and Richter [2]. For each modeling, the quality factor is deduced from the motional parameters of the equivalent electrical circuit. The higher Q

TABLE I

Frequency and quality factor for various radius of curvature

Rc [mm]	f [MHz]	Q
100	9.078	1 498 000
200	9.049	1 499 000
240	9.043	1 494 000
250	9.041	1 495 000
260	9.040	1 501 000
300	9.036	1 504 000
400	9.028	1 501 000

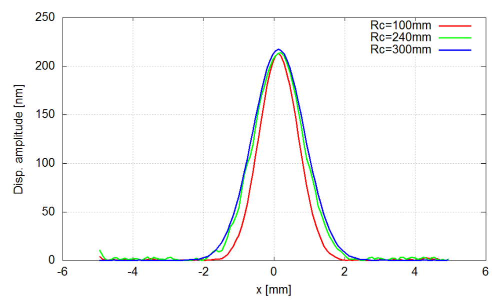

Fig. 2. Displacements within the resonator for 3 radii

and the best displacements are obtained when Rc is equal to 300 mm with Lm = 1.46 H and Rm = 55.2 Ω. We will use these data to compare the performances of the new designs.

III. Multi Mesa Resonator

We tested various configurations with several number and height of steps by ensuring that the discretization perfectly follows the chosen curvature as shown below.

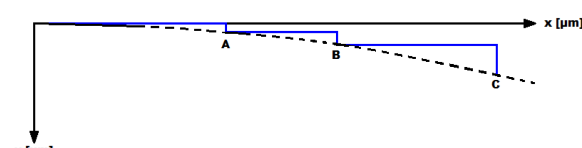

Fig. 3. Discretization of the curvature

The radius of curvature is represented in the figure 3 by the dotted line. The dimensions and the quality factor of new designs are summarized in the table II.

TABLE II

DIMENSIONS OF THE DIFFERENT DESIGNS IN MICROMETERS

Design	A(x,y)	B(x,y)	C(x,y)	D(x,y)	Q
1	(2500,10)	(3500,20)	(4500,33)	No	1 561 000
2	(2500,10)	(3500,20)	(4500,33)	(5500,50)	1 664 000
3	(3000,15)	(4000,27)	(5000,42)	No	1 586 000
4	(2500,10)	(3500,24)	(4500,72)	No	1 601 000
5	(2500,10)	(3500,24)	(4500,40)	(5500,72)	1 581 000
6	(3500,20)	(4500,33)	(5500,50)	No	1 524 000

As we can see in this table, in spite of a poor trapping of the vibrating energy (cf. Fig. 4 and 5), the quality factors are higher than those determined on a resonator owning a spherical surface.

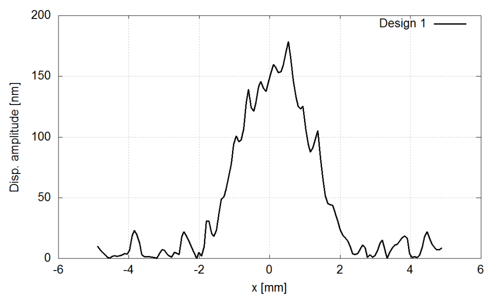

Fig. 4. Amplitude of displacements for design 1

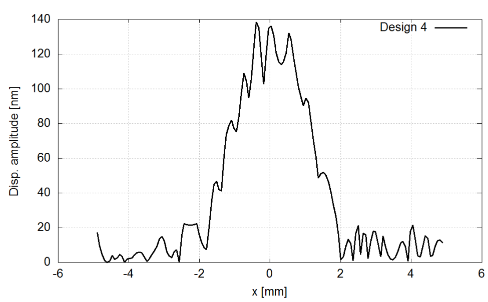

Fig. 5. Amplitude of displacements for design 4

Contrarily to the Fig. 2, the shape of the displacement curves is not perfect. We observe a lot of peaks which disturb the good trapping of the vibrating energy.

IV. PROGRESSIVE MESH

The thickness of the steps (and the elements within the mesas) is very small compared to the main part of the resonator. So, we have created a progressive mesh in order to avoid a possible discontinuity of mesh between the second mesa and the bulk which can be translated by a discrepancy on the final result. The height of the elements in the resonator will increase gradually to the opposite electrode.

This new mesh is created with COMSOL® by using the following algorithm [3] :

$$\sum_{i=1}^{e} \frac{i * r}{e * l} = L \tag{1}$$

where *L* is the total thickness of the resonator, *e* the number of elements, *r* the evolution ratio and *l* the length of the first layer. The equation (1) gives the value of *l* then we can determine the height of each element with :

$$h = \frac{i * r}{e * l} \tag{2}$$

By choosing the good ratio, the element near the last step will have the same thickness than those in the mesas. Various configurations have been tested with different ratio and number of elements in the bulk and steps. The results of the simulations are summarized in the table III. The dimensions of the resonator are identical to those of the design 1.

TABLE III

QUALITY FACTORS OBTAINED WITH PROGRESSIVE MESH

Design	Q	Lm [H]	Rm [H]
1.1	1 661 000	2.17	74.80
1.2	1 610 000	1.35	47.41
1.3	1 548 000	1.18	43.12
1.4	1 600 000	1.87	66.00
1.5	1 588 000	1.26	44.79
1.6	1 532 000	1.07	39.39
1.7	1 548 000	1.25	45.45
1.8	1 530 000	1.06	39.00

After testing several geometrical progressions, we succeed to improve the quality of the energy trapping (cf. Fig. 6 and 7). The displacement curves obtained with these two meshes are almost identical. The presence of peaks disturbing the trapping is less important than the design 1 (cf. Fig. 4).

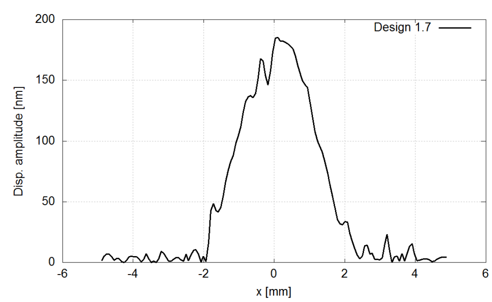

Fig. 6. Amplitude of displacements for design 1.7

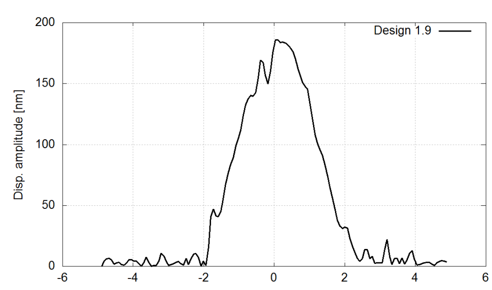

Fig. 7. Amplitude of displacements for design 1.9

But, despite a better trapping of the energy, the calculated quality factors are always too high compared to the "classical" resonator. By comparing the results determined with a radius of curvature with an internal software, we note that the value of the motional resistance is different between both whereas the inductance and the capacitance are very close. The quality factor being calculated with the motional parameters, the Q is not reliable to determine the best resonator design. So, we decided to refer only to the motional inductance (which translate the mechanical inertia) to select the optimal dimensions of the new resonator. As a reminder, the value of the inductance for a resonator with a radius of curvature of 300 mm is equal to 1.46 H (highest value that we choose as reference).

V. One step resonators

Modeling has been performed in order to study the behavior of resonators when the discretization is restricted to one step. For these simulations, the diameter of the mesa is equal to or bigger than the upper electrode. So, the electrical potential is only applied on one level in contrary to the previous computations.

TABLE IV
Results obtained for 1-step resonators

Design	A(x,y)	Lm [H]
1	(3500,20)	0.84
2	(4500,34)	0.63
3	(5500,50)	0.62

For each design, the discretization still follows the radius of curvature choosen in the section II.

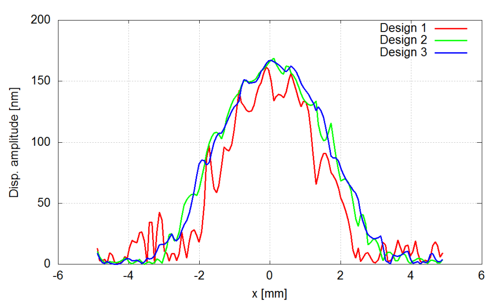

Fig. 8. Amplitude of displacements

By using only 1 mesa to discretize the radius of curvature, the value of the motional inductance decreases. Compared to the previous simulation, it is divided by 2 and it seems that the system has the same behavior as a plano-plano resonator and not as a plano-convex one. We also observe an improvement of the displacement curves when the diameter of the step is big. So, a high number of mesas would damage the trapping of the energy under the electrodes.

VI. Modeling of prototype

Following the previous results, we decided to realize a prototype for which the radius is discretize by two steps. The diameter of the smallest one should not be greater than the electrodes. The quality of these designs is evaluated only with the motional inductance and compared to the best value : 1.46 H (cf. Table I). The results of computations are summarized in the table V.

TABLE V
Frequency and inductance for 2-step prototypes

	∅ step 1	h step 1	∅ step 2	h step 2	f [MHz]	Lm [H]
1	5 mm	10 μm	7 mm	10 μm	8.976	1.55
2	3 mm	4 μm	7 mm	16 μm	8.990	1.57
3	6 mm	15 μm	8 mm	12 μm	8.971	1.00
4	5 mm	10 μm	9 mm	24 μm	8.975	1.04
5	6 mm	15 μm	7 mm	5 μm	8.972	1.14
6	4 mm	7 μm	6 mm	8 μm	8.984	1.56
7	5 mm	10 μm	11 mm	40 μm	8.974	1.17
8	4 mm	7 μm	7 mm	13 μm	8.983	1.45
9	5 mm	10 μm	7 mm	15 μm	8.976	1.88
10	5 mm	10 μm	7 mm	5 μm	8.977	1.37
11	3 mm	4 μm	7 mm	20 μm	8.989	1.28
12	3 mm	4 μm	7 mm	10 μm	8.990	1.24
13	5 mm	5 μm	7 mm	10 μm	8.974	0.98

We note that the design 8 gives the closest value to our reference while the prototype 13 is the most different (Lm = 0.98 H). The displacements obtained for these configurations are ploted in the figure 9.

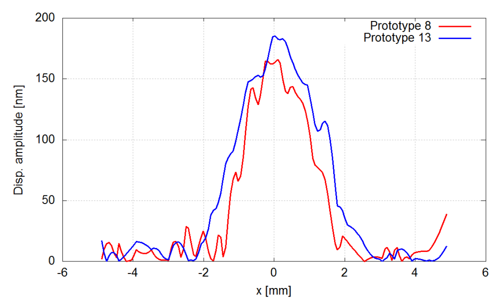

Fig. 9. Amplitude of displacements for the prototypes 8 and 13

For both, we did an eigenvalue analysis to search the position of some anharmonic spurious modes of the C-mode 3^{rd} overtone. The frequency of these several modes is summarized in the table VI.

TABLE VI
Frequencies of spurious modes

	Frequency [MHz]		
Mode	With curvature	Prototype 8	Prototype 13
C300	9.036	8.983	8.974
C320	9.144	---	---
C302	9.155	9.083	9.049
C340	9.254	9.157	9.133
C322	9.264	9.170	---
C304	9.276	9.175	9.149

Some of these anharmonic modes are not ”visible”, maybe due to the sparse mesh (used to decrease the computation time) or due to the choosen geometry. By calculating the shift between the main mode C300 and the spurious ones, we note that it is smaller for the prototype 13 than the 8. For example, there is a shift of 174 kHz between C300 and C340 while it is 159 kHz for the 13 (cf. Table VII).

TABLE VII
SHIFT BETWEEN THE MAIN MODE AND THE ANHARMONIC MODES

	Frequency shift [kHz]		
Mode	With curvature	Prototype 8	Prototype 13
C320	108	---	---
C302	118	100	75
C340	218	174	159
C322	228	187	---
C304	240	192	175

Compared to the resonator with radius of curvature, the evolution of the shift between C300 and the spurious modes is different for the prototype 8. It evolves from 218 kHz to 240 kHz for the high frequency modes (C340 and more) of the system with spherical surface while it is between 174 kHz and 192 kHz for the discretized resonator. We see with this table that the diameter of the smallest mesa has an effect on the position of these modes. If the diameter increases (e.g. prototype 13), the anharmonic modes get closer to the main one. So, the diameter of the first step of prototype 8 is maybe to big if we observe the frequency shift between this new design and the resonator with curvature.

VII. CONCLUSION

Though the trapping of the vibrating energy is not perfect, our first simulations gave high quality factors. So, in the goal of solving our problem, we have modified the mesh of the resonators in order to avoid the discontinuity of mesh between the second mesa (the largest) and the bulk. We succeed to improve the quality of the trapping but the Q is still too high compared to the ”classical” resonator. Then, we note that the calculation of the motional resistance (which is used to determine the quality factor) is probably biased. Nevertheless, we selected an optimum configuration with two steps for the new resonator by only refering to the motional inductance. Prototypes will be manufactured according to the dimensions determined by modeling (with radius of curvature and steps). Measurements on these prototypes will allow us to check our assumptions.

ACKNOWLEDGMENT

This work was funded by the ”Agence Nationale de la Recherche” in the framework of a french research project entitled ”FREQUENCE2009”.

REFERENCES

[1] J. Boy, H. Tavernier, X. Vacheret, T. Laroche, and A. Clairet, “Collective fabrication of 20 mhz resonators by deep reactive ion etching on 3” quartz wafers,” in *Joint Conference of the IEEE International Frequency Control and the European Frequency and Time Forum*, San Francisco, 2011.

[2] J. Lamb and J. Richter, “Anisotropic acoustic attenuation with new measurements for quartz at room temperatures,” *Proceedings of the Royal Society of London. Series A. Mathematical and Physical Sciences*, vol. 293, no. 1435, pp. 479–492, 1966.

[3] COMSOL® Support.